Abdominal Radiology (2019) 44:2366–2376
https://doi.org/10.1007/s00261-019-01968-7

HEPATOBILIARY

Diagnosis of recurrent HCC: intraindividual comparison of gadoxetic acid MRI and extracellular contrast-enhanced MRI

Jae Hyun Yim[1] · Young Kon Kim[1] · Ji Hye Min[1,2] · Jisun Lee[3] · Tae Wook Kang[1] · Soon Jin Lee[1]

Published online: 8 March 2019

Abstract

Purpose To compare the efficacy of magnetic resonance imaging (MRI) with hepatobiliary agents (HBA-MRI) and MRI with extracellular contrast agents (ECA-MRI) for detection of recurrent hepatocellular carcinoma (HCC) after multiple treatments.

Methods The institutional review board approved this retrospective study and waived the requirement for informed patient consent. A total of 135 patients with suspected HCC recurrence after 2–5 treatments (surgery, transarterial chemoembolization, and/or radiofrequency ablation) underwent both HBA-MRI and ECA-MRI within a 1 month interval. HBA-MRI and ECA-MRI were analyzed for HCC detection by two observers using a five-point scale. The diagnostic performances according to MRI modality were compared.

Results A total of 136 liver lesions (121 HCCs and 15 benign lesions; median size, 1.9 cm) were identified. ECA-MRI showed greater sensitivity (90.9% vs. 76.9% for observer 1; 91.7% vs. 78.5% for observer 2) and accuracy (91.2% vs. 78.7% for observer 1; 91.9% vs. 80.2% for observer 2) than HBA-MRI for both observers ($P = 0.002$, 0.003). Fifteen (12.4%) HCCs were correctly diagnosed with ECA-MRI but not with HBA-MRI by both observers. Interobserver agreement was excellent (0.885) for ECA-MRI and substantial (0.749) for HBA-MRI.

Conclusions For detection of recurrent HCC, ECA-MRI was superior to HBA-MRI in terms of sensitivity and accuracy. Therefore, ECA-MRI could be the preferred imaging modality over HBA-MRI for assessing HCC recurrence following multiple treatments.

Keywords Liver · Hepatocellular carcinoma · Magnetic resonance imaging · Contrast agents · Recurrence

Abbreviations

MRI	Magnetic resonance imaging
HBA	Hepatobiliary agents
ECA	Extracellular contrast agents
HCC	Hepatocellular carcinoma
CT	Computed tomography
Gd-EOB-DTPA	Gadolinium-ethoxybenzyl-diethylene-triamine pentaacetic acid
LI-RADS	Liver Reporting and Data System
HBP	Hepatobiliary phase
TP	Transitional phase
PVP	Portal venous phase
T2WI	T2-weighted image
DWI	Diffusion-weighted image
ROC	Receiver operating characteristics
AUC	Under the ROC curve
PPV	Positive predictive value
NPV	Negative predictive value
RFA	Radiofrequency ablation
TACE	Transarterial chemoembolization

Electronic supplementary material The online version of this article (https://doi.org/10.1007/s00261-019-01968-7) contains supplementary material, which is available to authorized users.

✉ Young Kon Kim
youngkon0707.kim@samsung.com; jmyr@dreamwiz.com

[1] Present Address: Department of Radiology and Center for Imaging Science, Samsung Medical Center, Sungkyunkwan University School of Medicine, 81 Irwon-ro, Gangnam-gu, Seoul, Republic of Korea

[2] Department of Radiology, Chungnam National University Hospital, Chungnam National University College of Medicine, Daejeon, Republic of Korea

[3] Department of Radiology, Chungbuk National University Hospital, Cheongju, Republic of Korea

Introduction

With technical breakthroughs in cross-sectional liver imaging using computed tomography (CT) and magnetic resonance imaging (MRI), diagnosis of hepatocellular carcinoma (HCC) is possible without histology, based on arterial hyperenhancement followed by washout [1–5]. HCC diagnostic criteria are derived from vascular profiles based on dynamic CT or MRI using extracellular contrast agent (ECA) [1, 2, 4, 5]. Now, with widespread use of the hepatobiliary agent (HBA) [6, 7], gadolinium-ethoxybenzyl-diethylenetriamine pentaacetic acid (Gd-EOB-DTPA; Primovist®), imaging features based on MRI using HBA (HBA-MRI) have been adopted by some organizations, including Asian groups and the Liver Reporting and Data System (LI-RADS) [8, 9].

Current HCC diagnostic criteria typically refer to an initially detected hepatic nodule in patients with no prior HCC treatment. Current criteria, based on conventional hemodynamic information alone, offer close to 100% specificity, but have limited sensitivity, as 30–40% of HCC do not meet the criteria, particularly for small tumors (< 20 mm) [3]. The strongpoint of Gd-EOB-DTPA is delineation of liver lesions as areas of hypointense defects against a strongly enhanced adjacent liver parenchyma in hepatobiliary phase (HBP) images. The improved contrast leads to improved sensitivity for HCC diagnosis, as well as additional tumor detection [10]. However, a concern of applying hypointensity on transitional phase (TP) or HBP as a diagnostic criterion is that non-HCC hypervascular hepatic tumors might be misclassified as HCC, since Gd-EOB-DTPA is taken up by hepatocytes starting at 90 s following contrast injection [11]. Thus, according to LI-RADS, when Gd-EOB-DTPA is used, "washout" refers to the portal venous phase (PVP) prior to the TP [12–15]. However, when assessing tumor recurrence following HCC treatment, HCC criteria with high sensitivity are desirable, as newly developed hepatic nodules are likely to be HCC.

In that sense, we hypothesized that HBA-MRI would show superior diagnostic performance over ECA-MRI, considering the high sensitivity to detect HCC as HBP hypointensity. However, there have been no well-validated studies on imaging criteria or choice of MRI contrast agent for diagnosing recurrent HCC, and to the best of our knowledge, there have been no direct comparisons of ECA-MRI and HBA-MRI for recurrent HCC diagnosis. Therefore, we conducted this study to compare the performance of ECA-MRI and HBA-MRI in diagnosing recurrent HCC in an intra-individual, cross-over manner.

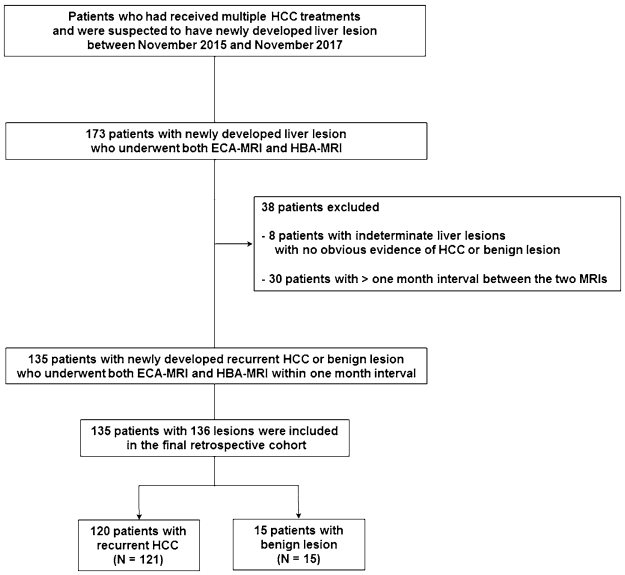

Fig. 1 Flow diagram for our study

Materials and methods

Patients

Our Institutional Review Board approved this retrospective study and waived the need for informed consent. Between November 2015 and November 2017, 173 patients who had received multiple HCC treatments and were suspected to have newly developed liver lesion underwent both ECA-MRI and HBA-MRI at Samsung Medical Center, Seoul, Korea. Our institution prefers HBA-MRI to maximize the detection sensitivity for focal liver lesion. However, if a possible recurrent HCC is revealed by HBA-MRI under a clinical situation of which the decision of whether or not to perform immediate treatment is challenging (for example, in a patient with poor hepatic reservoirs), an additional ECA-MRI was conducted to acquire a full-scale imaging examination. In addition, ECA-MRI was obtained in the radiation therapy planning process to compensate for liver motion with breathing [16].

The inclusion criteria for this intraindividual comparison of the two MRIs were (1) recurrent HCC (local tumor recurrence at a previously treated area or intrahepatic metastasis) or a newly developed benign liver lesion after HCC treatments and (2) HBA-MRI and ECA-MRI performed within 1 month interval (mean interval, 15 days; range 9–30 days). Patients with indeterminate liver lesions with no obvious evidence of HCC or benign lesion ($n = 8$) and those with more than 1 month interval between the two MRIs ($n = 30$) were excluded from the study. Consequently, 135 patients (108 men, 27 women; age range,

32-76 years) with chronic hepatitis or cirrhosis were included (Fig. 1).

Reference standards

Reference standard for recurrent HCC was based on the clinical criteria, thoroughly evaluated by one radiologist (Y. K. K. with 18 years of abdominal imaging experience). The clinical diagnosis of HCC was based on histopathological examination of the surgical specimens ($n=3$) or its typical imaging hallmarks (arterial hyperenhancement and washout) on CT and also on either of the two MRIs [1–3, 17, 18]. If HCC could not be diagnosed due to discordant finding on CT and MRIs, the following features were considered diagnostic for HCC within 6 months after the imaging: increase in size (with increasing trend of serum alpha-fetoprotein in patients with suppressed hepatitis activity) or a change in the enhancement pattern (hypervascularization in a previously non-hypervascular nodule or washout in a nodule with initial arterial hypervascularization but without washout) [18]. Size increase of a hepatic lesion was defined by threshold growth by LI-RADS v2017. The diagnosis of benign lesion was based on percutaneous biopsy ($n=1$) or imaging findings of stability or reduced lesion size without treatment during at least 12 months of follow-up.

MRI examinations

MRI examinations were performed using a 3.0T MR system (Intera Achieva 3.0T, Philips Healthcare, Best, Netherlands) equipped with a dual-source parallel radiofrequency transmission system and quadrature body coil. Baseline MRI included a T1-weighted turbo field echo in- and opposed-phase sequence, breath-hold multishot T2-weighted image (T2WI), and respiratory-triggered heavily T2WI. Diffusion-weighted image (DWI) was performed using respiratory-triggered single-shot echo-planar imaging with b-values of 0, 100, and 800 s/mm^2. In contrast-enhanced imaging, unenhanced, arterial-phase (25-30 s), portal-phase (60 s), 3-min delayed-phase (TP in HBA-MRI), and 20-min HBP (only after Gd-EOB-DTPA administration) images were obtained using a T1-weighted 3D turbo field echo sequence (T1 high-resolution isotropic volume examination; THRIVE, Philips Healthcare). The time used for arterial phase imaging was determined using an MR fluoroscopic bolus detection technique. Contrast agent was administered intravenously using a power injector at a rate of 1 mL/s for a dose of 0.025 mmol/kg body weight for Gd-EOB-DTPA) or a rate of 2 mL/s for a dose of 0.1 mmol/kg body weight for the extracellular gadolinium contrast agent gadoterate meglumine (Gd-Dota, Dotarem®; Guerbet, France), followed by a 20 mL saline flush. Detailed parameters of the MR sequences used are summarized in Table S1.

Image analysis

All MRI features were evaluated in two separate sessions by two gastrointestinal radiologists (T. W. K. and J. H. M., with 12 and 11 years of experience in interpreting liver MRIs, respectively) who were blinded to the final diagnoses in an anonymized and randomized manner. To minimize learning bias, there was a four-week interval between interpretations. Observers were allowed to review the prior image for localization of preexisting benign liver lesions such as hemangioma or of treated areas.

The observers knew that patients were at risk for intrahepatic HCC recurrence (either local tumor progression or intrahepatic metastasis). Two observers reviewed the MRIs and indicated confidence levels as follows: 1, definitely benign; 2, probably benign; 3, intermediate lesion; 4, probably HCC; 5, definitely HCC. The definitions of each point on the scale were listed in Table 1. Category 5 (definitely HCC) was defined as nodules with a focal, discrete, nodular arterial hyperenhancement, and washout on PVP and/or delayed

Table 1 Definition of confidence level according to the five-point scale

Score	Definition	
	ECA-MRI	HBA-MRI
1, Definitely benign	Lesions not detected in each MRI	
2, Probably benign	No arterial hyperenhancement	
3, Intermediate	Assigned to category 2 or 3 according to the shape and conspicuity of the lesion in other MR sequences	
4, Probably HCC	Arterial hyperenhancement with hyperintensity on T2WI and DWI	
	No washout on PVP and delayed phase	No washout on PVP No hypointensity on TP and HBP
5, Definitely HCC	Focal, discrete, nodular arterial hyperenhancement	
	Washout on PVP and/or delayed phase	Washout on PVP and/or hypointensity on TP and/or HBP[a]

[a]Hypointensity on TP and/or HBP on HBA-MRI as an alternative to washout when accompanying clear hyperintensity on T2WI and/or DWI

phase on ECA-MRI or washout on PVP on HBA-MRI. We considered hypointensity on TP and/or HBP on HBA-MRI as an alternative to washout when accompanying clear hyperintensity on T2WI and/or DWI, taking into account the clinical setting in which newly developed hepatic nodules following HCC treatment are likely to be HCC. Category 4 (probably HCC) was defined as nodules showing arterial hyperenhancement with hyperintensity on T2WI and DWI, but neither washout nor HBP hypointensity. When lesions showed no arterial hyperenhancement, they were assigned to category 2 or 3 according to the shape and conspicuity of the lesion in other MR sequences. Lesions not detected by each MRI were assigned to category 1. Because these criteria provided rough reference standards to the observers, the final decision was made by subjective judgment based on each observer's clinical experience.

Statistical analysis

Continuous variables were compared parametrically using the Mann–Whitney U test. Categorical variables were compared using the x^2 test or Fisher's exact test, as appropriate.

The diagnostic performance of each observer was calculated with a receiver operating characteristics (ROC) curve analysis, and the area under the ROC curve (AUC) was calculated. For comparing the diagnostic performance between two MRIs, pairwise comparisons of the ROC curves were performed. The 95% confidence intervals (CI) were used to express the statistical precision of the results. Regarding the recurrent HCCs, the sensitivity for each MRI was evaluated according to the number of lesions assigned a confidence level of 4 or 5. For each MRI, we calculated sensitivity, specificity, accuracy, positive predictive value (PPV), and negative predictive value (NPV). McNemar's test with continuity correction was used to compare the sensitivity, specificity, and accuracy of two MRIs, and Bennett's test was used to compare the PPV and NPV of the two MRIs [19]. For comparison of diagnostic performance of pooled data, we used the GEE (generalized estimating equation) method due to possible influence of lesion clustering on diagnostic accuracy. Inter-reviewer agreement for assessing MR imaging was analyzed using the kappa statistic, with 0.8–1.0 considered excellent agreement; 0.6–0.79, substantial agreement; 0.4–0.59, moderate; 0.2–0.39, fair; 0.1–0.19, slight; and 0–0.1, poor agreement [20].

We conducted a power analysis to determine the sample size required for this superiority study. We assumed a liver malignancy detectability of 87% using HBA-MRI based on previous study [21] and expected a superiority margin of 10% and a detectability of 97% for ECA-MRI. Based on these assumptions, a sample size of 120 HCCs was calculated to give 90% statistical power with a two-sided alpha value of 0.05, with 12% expected discordant pairs between the two MR examinations [22]. $P < 0.05$ was considered significant. Statistical analysis was executed using SAS version 9.4 (SAS Institute, Cary, NC) and R 3.4.1 (Vienna, Austria).

Results

Patient and lesion characteristics

The patient and lesion characteristics are described in Table 2. Among 135 patients, 102 (75.6%) patients were classified as Child–Pugh class A and 33 (24.4%) as Child–Pugh class B. All patients received multiple treatments (range 2–5; mean, 3.4); 10 (7.4%) patients received two treatments, 70 (51.9%) patients received three, 42 (31.1%) patients received four, and 13 (9.6%) received five treatments. Prior HCC treatments were as follows: hepatic resection for 28 (20.7%) patients, radiofrequency ablation (RFA) for 88 (65.2%) patients, and transarterial chemoembolization (TACE) for 115 (85.2%) patients (Figs. 2, 3 and 4). Among 135 patients, one patient had two HCCs; all other patients had one index lesion. A total of 136 hepatic lesions included 121 (89.0%) HCCs (size range, 0.8–5.0 cm; median, 1.9 cm) and 15 (11.0%) benign lesions including 10 (7.4%) arterioportal shunts and five (3.7%) inflammations such as eosinophilic infiltration (size range, 0.8–2.5 cm; median, 1.8 cm). Of the 121 recurrent HCCs, 30 (24.8%) were 0.8–1.0 cm in diameter (Fig. 3), 68 (56.2%) were 1.1–2.0 cm, and 23 (19.0%) were ≥ 2.0 cm. Of the 121 recurrent HCCs, 62 (51.2%) lesions were local tumor recurrence at prior treatment area after TACE (Fig. 2) or RFA, 59 (48.8%) lesions were intrahepatic metastasis located in the same segment ($n = 32$) or lobe ($n = 24$) harboring a prior treatment area, and three (2.5%) lesions were in the contralateral lobe (Fig. 3).

Diagnostic performance for detection of recurrent HCC

In the detection of recurrent HCCs, the AUC values for ECA-MRI showed significantly superior to that of HBA-MRI in both observers (0.978 vs. 0.933 for observer 1; 0.976 vs. 0.923 for observer 2; $P = 0.015$ and 0.009) (Table 3 and Fig. 5). In addition, the ECA-MRI was superior to HBA-MRI for detecting recurrent HCC in terms of sensitivity (90.9% vs. 76.9% for observer 1; 91.7% vs. 78.5% for observer 2; $P = 0.002$ and 0.003) and accuracy (91.2% vs. 78.7% for observer 1; 91.9% vs. 80.2% for observer 2; $P = 0.002$ and 0.003). In addition, ECA-MRI achieved higher NPV (56.0% for observer 1; 58.3% for observer 2) than HBA-MRI (33.3% for observer 1; 35.0% for observer 2) ($P = 0.020$ and 0.023) (Table 3). The number of HCCs correctly diagnosed on ECA-MRI and not diagnosed on

Table 2 Patient and lesion characteristics

	Patients with recurrent HCC (N = 120)	Patients with benign lesion (N = 15)	*P* value
Demographic features			
Age (years)[a]	62.5 (34–85)	67.0 (45–85)	0.455
Sex			1.000
Male	96 (78.3)	12 (80.0)	
Female	26 (21.7)	3 (20.0)	
Underlying liver disease			0.914
Hepatitis B	85 (70.8)	10 (66.7)	
Hepatitis C	23 (19.2)	3 (20.0)	
Others	12 (10.0)	2 (13.3)	
Liver cirrhosis	108 (87.5)	12 (80.0)	0.423
Child–Pugh classification			0.760
A	91 (75.8)	11 (73.3)	
B	29 (24.2)	4 (26.7)	
AFP level (ng/mL)[a]	12.1 (1.8–24563.3)	5.2 (1.3–293.3)	<0.001
Lesions	N = 121[b]	N = 15	
Size (cm)[a]	1.9 (0.8–5.0)	1.8 (0.8–2.5)	0.023
Size subgroup			0.978
≤ 1.0 cm	30 (24.8)	4 (26.7)	
1.1–2.0 cm	68 (56.2)	8 (53.3)	
> 2.0 cm	23 (19.0)	3 (20.0)	
Type of recurrence			–
Local tumor recurrence	62 (51.2)	–	
Intrahepatic metastasis	59 (48.8)	–	
Same segment	32 (26.5)	–	
Same lobe	24 (19.8)	–	
Contralateral lobe	3 (2.5)	–	

Except where indicated, numbers in parentheses are percentages

HCC hepatocellular carcinoma, *AFP* alpha-fetoprotein

[a]Data are presented as median (range)

[b]121 recurrent HCCs in 120 patients

HBA-MRI was 20 (16.5%) for observer 1 and 19 (15.7%) for observer 2, with 15 (12.4%) common to both observers (Tables S2 and S3, Fig. 2). Thirteen of these 15 HCCs were seen in patients with a history of repeated TACE (≥ two treatments; range 2–5) (Fig. 4). Ten of these 15 HCCs were seen in patients with Child–Pugh class B. In the retrospective review, they were observed as a hypovascular nodule without arterial hyperenhancement on HBA-MRI ($n = 9$) (Fig. 3) or as arterially enhancing nodules with neither washout nor hypointensity on HBP ($n = 6$). Only three (2.5%) HCCs were correctly diagnosed on HBA-MRI but not on ECA-MRI, by both observers. Seven (5.8%) HCCs were not discerned by either observer.

One benign lesion was misdiagnosed as recurrent HCC by both observers on both ECA-MRI and HBA-MRI. Thus, the two MRIs showed the same specificity (93.3%, 14/15). PPVs showed no significant difference between the two MRIs for both observers ($P = 0.672$, 0.675) (Table 3 and Table S2).

Pooled data for the two observers (Table 3) also showed higher sensitivity and accuracy for ECA-MRI (91.3% and 91.5%, respectively) than HBA-MRI (77.7% and 79.4%; $P < 0.001$). In addition, ECA-MRI showed a significantly higher NPV than HBA-MRI (57.1% vs. 34.1%; $P < 0.001$).

Interobserver agreement

The kappa values between the two observers were 0.885 for ECA-MRI and 0.749 for HBA-MRI, indicating excellent and substantial interobserver agreement, respectively, with regard to intrahepatic HCC recurrence.

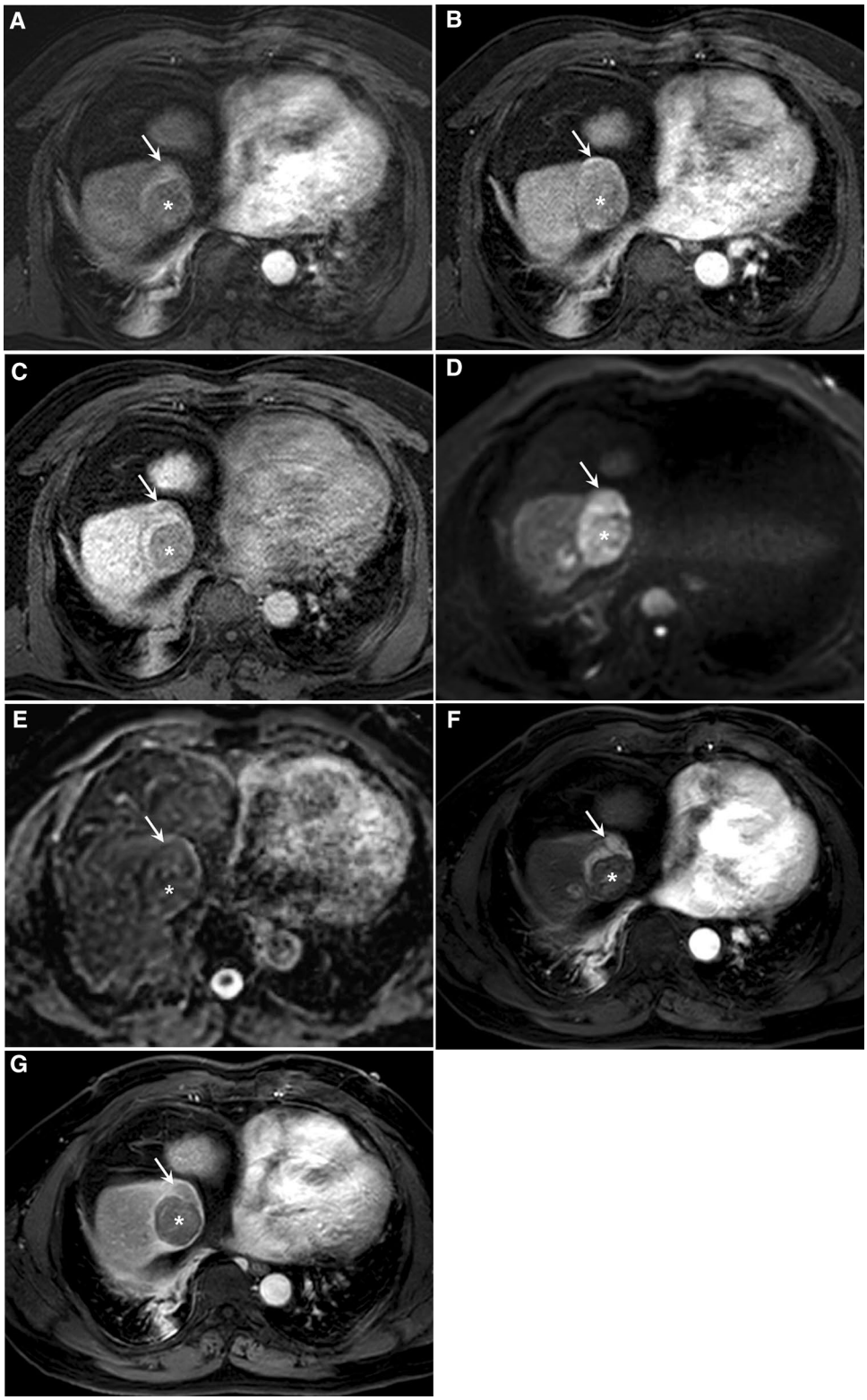

Fig. 2 Recurrent hepatocellular carcinoma in a 57-year-old male with a history of repeated transarterial chemoembolization. **a** Arterial phase, **b** portal venous phase, and **c** 20-min hepatobiliary phase images following Gd-EOB-DTPA administration. Arterial hyperenhancement (arrow) is suspected at the margin of a previously treated area (asterisk), but neither washout nor hepatobiliary hypointensity is clearly discerned. **d** Diffusion-weighted image (b-800) and **e** ADC map, in which a recurrent tumor is not clearly discerned from the previously treated area (asterisk). **f** Arterial phase and **g** portal venous phase after administration of extracellular contrast agent. A marginal tumor recurrence is clearly delineated as an arterial hyperenhancing area, followed by washout (arrow)

Discussion

This study demonstrates that ECA-MRI allows greater sensitivity and accuracy than HBA-MRI for diagnosis of recurrent HCC. The clinical setting in which newly developed hepatic nodules following HCC treatment are likely to be HCC regardless of size requires the HCC diagnostic criteria to be reformed; for example, by incorporating

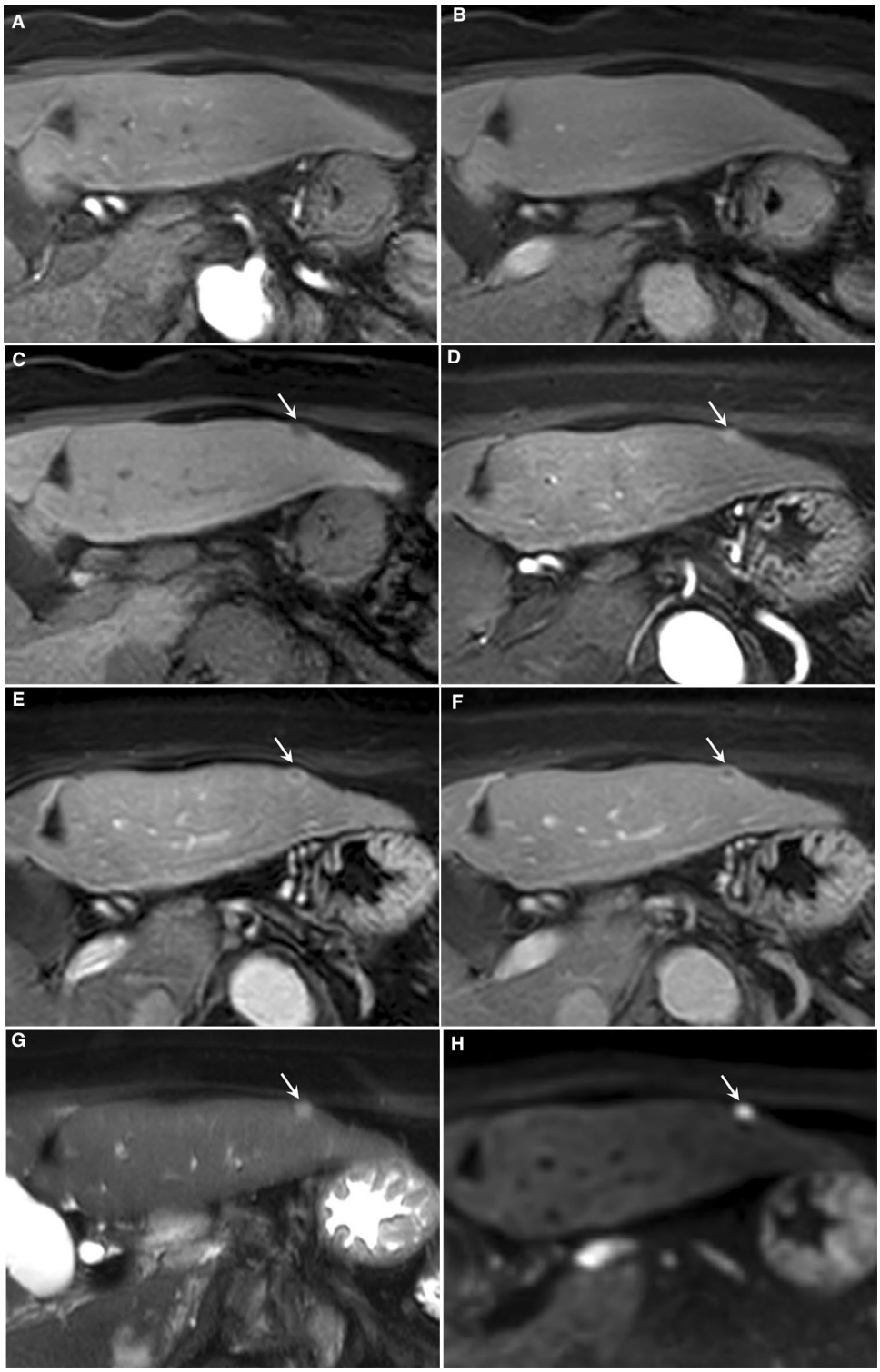

Fig. 3 Recurrent hepatocellular carcinoma in an 80-year-old woman with a history of repeated transarterial chemoembolization. **a** Arterial phase, **b** portal venous phase, and **c** and 20-min hepatobiliary phase images after Gd-EOB-DTPA administration. Arterial hyperenhancement or portal washout is not clearly seen, and a hypointense nodule (arrow) is observed on hepatobiliary phase. **d** Arterial phase, **e** portal venous phase, and **f** delayed phase after administration of extracellular contrast agent. A small tumor is clearly detectable as arterial hyperenhancement and washout with capsular enhancement (arrows). **g** T2-weighted image and **h** diffusion-weighted image (b-800). A recurrent tumor clearly shows hyperintensity

imaging features considered ancillary features of HCC in LI-RADS (e.g., hypointensity on HBP or TP and hyperintensity on T2WI or DWI) [8]. As we hypothesized, it is generally expected that HBA-MRI would outperform ECA-MRI if stringent HCC guidelines that prioritize specificity over sensitivity are not applied [2, 4, 5, 10], due to the high sensitivity of HBP to detect HCC as hypointense. Our results run counter to this expectation.

There are several possible explanations for the superior diagnostic performance of ECA-MRI over HBA-MRI in recurrent HCC diagnosis in our study. Of 15 HCCs correctly diagnosed with ECA-MRI but not with HBA-MRI

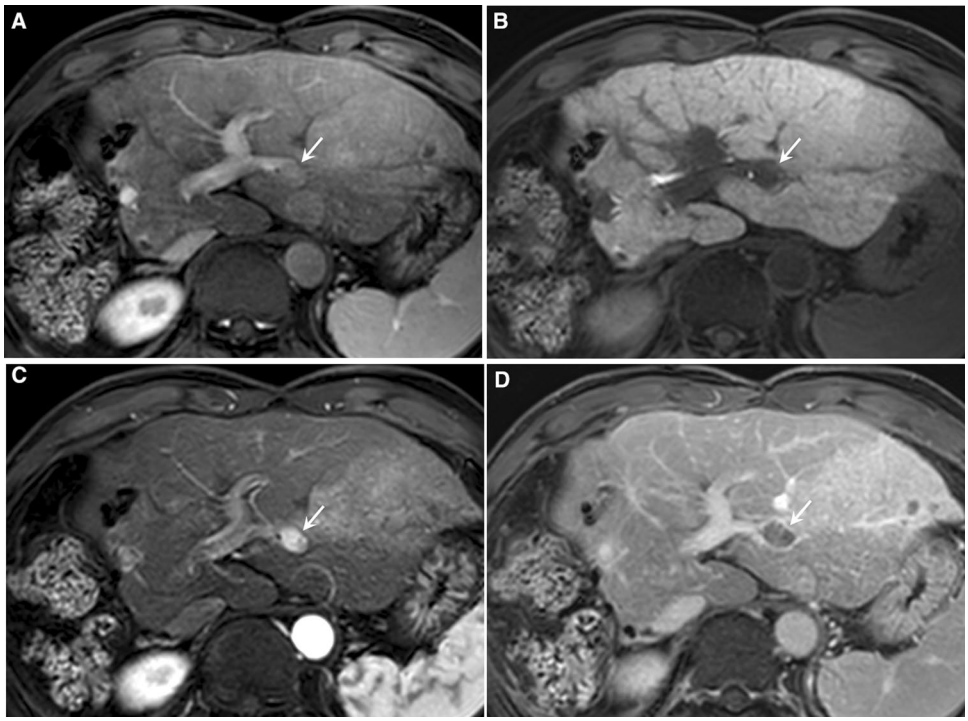

Fig. 4 Recurrent hepatocellular carcinoma in a 56-year-old male with a history of repeated transarterial chemoembolization and hemihepatectomy. **a** Arterial phase and **b** 20-min hepatobiliary phase images after Gd-EOB-DTPA administration. A recurrent tumor (arrows) is not clearly discerned due to overlapping with portal vein. **c** Arterial phase and **d** delayed phase after administration of extracellular contrast agent. A recurrent tumor clearly shows arterial hyperenhancement and washout with capsular enhancement (arrows)

Table 3 Comparison of diagnostic performance for recurrent HCC between ECA-MRI and HBA-MRI

	ECA-MRI			HBA-MRI			*P* value
	Value	95% CI		Value	95% CI		
Observer 1							
Area under ROC curve	0.978	0.936	1.000	0.933	0.868	0.997	0.015
Accuracy (%)	91.2 (124/136)	84.2	95.3	78.7 (107/136)	69.9	85.5	0.002*
Sensitivity (%)	90.9 (110/121)	83.3	95.2	76.9 (93/121)	67.3	84.3	0.002*
Specificity (%)	93.3 (14/15)	65.9	99.0	93.3 (14/15)	65.9	99.0	N/A
PPV (%)	99.1 (110/111)	94.1	99.9	98.9 (93/94)	93.1	99.9	0.672†
NPV (%)	56.0 (14/25)	34.7	75.3	33.3 (14/42)	19.6	50.6	0.020†
Observer 2							
Area under ROC curve	0.976	0.935	1.000	0.923	0.857	0.988	0.009
Accuracy (%)	91.9 (125/136)	85.1	95.8	80.2 (109/136)	71.5	86.7	0.003*
Sensitivity (%)	91.7 (111/121)	84.3	95.8	78.5 (95/121)	69.1	85.7	0.003*
Specificity (%)	93.3 (14/15)	65.9	99.0	93.3 (14/15)	65.9	99.0	N/A
PPV (%)	99.1 (111/112)	94.1	99.9	99.0 (95/96)	93.2	99.9	0.675†
NPV (%)	58.3 (14/24)	36.3	77.4	35.0 (14/40)	20.7	52.7	0.023†
Pooled data							
Area under ROC curve	0.979	0.944	1.000	0.937	0.881	0.993	0.011‡
Accuracy (%)	91.5 (249/272)	87.6	94.3	79.4 (216/272)	74.2	83.8	< 0.001‡
Sensitivity (%)	91.3 (221/242)	87.1	94.3	77.7 (188/242)	72.0	82.5	< 0.001‡
Specificity (%)	93.3 (28/30)	78.7	98.2	93.3 (28/30)	78.7	98.2	N/A
PPV (%)	99.1 (221/223)	96.8	99.9	98.9 (188/190)	96.2	99.7	< 0.001‡
NPV (%)	57.1 (28/49)	43.3	70.0	34.2 (28/82)	24.8	44.9	< 0.001‡

HCC hepatocellular carcinoma, *MRI* magnetic resonance imaging, *ECA* extracellular agent, *HBA* hepatobiliary agent, *CI* confidence interval, *ROC* receiver operating characteristic, *PPV* positive predictive value, *NPV* negative predictive value, *N/A* not applicable

*McNemar's test, †Bennett's test, ‡Generalized estimating equation

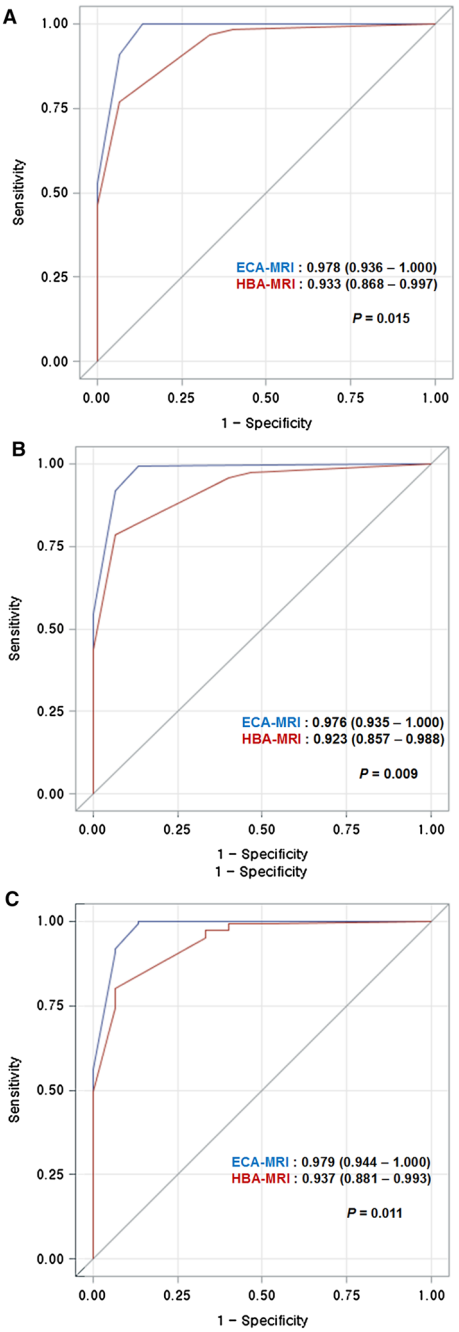

Fig. 5 ROC curves for diagnostic performance for recurrent HCC by two observers according to MRI modality, **a** Observer 1, **b** Observer 2, and **c** Pooled data

by both observers, 13 were in patients with a history of repeated TACE treatment, which may have caused injury of the hepatic artery and poor arterial supply in the treated area of the liver [23, 24]. In fact, nine of them observed as hypovascular nodule without arterial hyperenhancement on HBA-MRI. Liver injury due to TACE treatment could hamper delineation of arterial hyperenhancement, particularly for small HCCs [25, 26], (Fig. 3) to a greater extent in HBA-MRI than in ECA-MRI (Figs. 2, 3, and 4), considering the lower recommended dosage for Gd-EOB-DTPA vs. ECA (0.025 vs. 0.1 mmol/kg) [27]. In addition, the decreased dose in administered volume of HBA can create difficulty to acquire the optimal late arterial phase that is essential for visualizing hyperenhancement of HCC. Of the 121 recurrent HCCs, 62 (51.2%) lesions were at a marginal area of a prior treatment such as TACE or RFA, and 56 (46.3%) lesions were located in the treated segment or hepatic lobe. Arterial hypervascularization was the most important HCC criterion used in our study. The majority of lesions, even subcentimeter lesions, demonstrated arterial hypervascularization without evidence of a premalignant lesion in a prior MRI examination, indicating intrahepatic metastasis rather than multicentric HCC recurrence.

Another possible explanation for the superiority of ECA-MRI to HBA-MRI in our study is that repeated treatments may have worsened hepatic dysfunction and reduced lesion conspicuity on HBP (in HBA-MRI) due to reduced enhancement of background liver parenchyma [28]. In addition, since treated areas are seen as hypointense areas on HBP regardless of tumor viability, HBP might have no benefit in delineation of marginal recurrence unless arterial hyperenhancement is clearly seen (Fig. 4). In contrast, for ECA-MRI, during PVP or delayed phase, the washout area of viable tumors tends to be brighter than the treated area (Fig. 2). However, smaller HCCs are less likely to show washout than larger ones [29]. The presence of mild to moderate hyperintensity on T2WI or diffusion restriction could be useful in characterizing arterial hyperenhancing nodules without washout as being true HCC or pseudolesion [10, 13, 26]. In LI-RADS, T2 hyperintensity or diffusion restriction is considered an ancillary finding, with which lesions could be assigned up to LR-4 (possibly HCC) [8].The treatment strategy for HCC recurrences after multiple treatments would be different from a newly-detected HCC that might warrant consideration of transplantation. Thus, HCC criteria for recurrence do not need to be congruent with current HCC criteria that prioritize high specificity, as proposed by the American Association for the Study of Liver Disease and the European Association for the Study of the Liver [2, 4, 5]. Accordingly, ancillary findings such as T2 hyperintensity or diffusion restriction could be used as an alternative to washout or hypointensity on TP and HBP in assessing recurrent HCC.

This study had several limitations. First, the retrospective nature of the study may have introduced inherent selection bias. Our patient cohort may have been biased by the large number of patients who received repeated treatments, most commonly TACE and then RFA. Second, all patients first underwent HBA-MRI and then ECA-MRI according to the clinician's decision. Thus, our patient cohort might be biased toward hepatic lesions that were difficult to assess

using HBA-MRI. In addition, the pre-test probability is high because a new lesion of any pattern is likely to be a new HCC. Therefore, this study included a large number of HCCs and a relatively small number of benign cases, impacting statistical analysis. Finally, the reference standard for HCC diagnosis was a composite, consisting mostly of imaging features.

Conclusions

For detection of HCC recurrence in patients with a history of multiple treatments, ECA-MRI showed better sensitivity and accuracy than HBA-MRI. Therefore, ECA-MRI could be the preferred imaging modality over HBA-MRI for assessing HCC recurrence following multiple treatments.

References

1. Bruix J, Sherman M (2011) Management of hepatocellular carcinoma: an update. Hepatology 53:1020-1022. https://doi.org/10.1002/hep.24199
2. (2012) EASL-EORTC clinical practice guidelines: management of hepatocellular carcinoma. J Hepatol 56:908-943. https://doi.org/10.1016/j.jhep.2011.12.001
3. Forner A, Vilana R, Ayuso C, Bianchi L, Sole M, Ayuso JR, Boix L, Sala M, Varela M, Llovet JM, Bru C, Bruix J (2008) Diagnosis of hepatic nodules 20 mm or smaller in cirrhosis: Prospective validation of the noninvasive diagnostic criteria for hepatocellular carcinoma. Hepatology 47:97-104. https://doi.org/10.1002/hep.21966
4. Heimbach JK, Kulik LM, Finn RS, Sirlin CB, Abecassis MM, Roberts LR, Zhu AX, Murad MH, Marrero JA (2018) AASLD guidelines for the treatment of hepatocellular carcinoma. Hepatology 67:358-380. https://doi.org/10.1002/hep.29086
5. (2018) EASL Clinical Practice Guidelines: Management of hepatocellular carcinoma. J Hepatol 69:182-236. https://doi.org/10.1016/j.jhep.2018.03.019
6. Kim YK, Kim CS, Han YM, Yu HC, Choi D (2011) Detection of small hepatocellular carcinoma: intraindividual comparison of gadoxetic acid-enhanced MRI at 3.0 and 1.5 T. Invest Radiol 46:383-389. https://doi.org/10.1097/RLI.0b013e318217b8fb
7. Sun HY, Lee JM, Shin CI, Lee DH, Moon SK, Kim KW, Han JK, Choi BI (2010) Gadoxetic acid-enhanced magnetic resonance imaging for differentiating small hepatocellular carcinomas (< or =2 cm in diameter) from arterial enhancing pseudolesions: special emphasis on hepatobiliary phase imaging. Invest Radiol 45:96-103. https://doi.org/10.1097/RLI.0b013e3181c5faf7
8. Elsayes KM, Hooker JC, Agrons MM, Kielar AZ, Tang A, Fowler KJ, Chernyak V, Bashir MR, Kono Y, Do RK, Mitchell DG, Kamaya A, Hecht EM, Sirlin CB (2017) 2017 Version of LI-RADS for CT and MR Imaging: An Update. Radiographics 37:1994-2017. https://doi.org/10.1148/rg.2017170098
9. Omata M, Cheng AL, Kokudo N, Kudo M, Lee JM, Jia J, Tateishi R, Han KH, Chawla YK, Shiina S, Jafri W, Payawal DA, Ohki T, Ogasawara S, Chen PJ, Lesmana CRA, Lesmana LA, Gani RA, Obi S, Dokmeci AK, Sarin SK (2017) Asia-Pacific clinical practice guidelines on the management of hepatocellular carcinoma: a 2017 update. Hepatol Int 11:317-370. https://doi.org/10.1007/s12072-017-9799-9
10. Choi JY, Lee JM, Sirlin CB (2014) CT and MR imaging diagnosis and staging of hepatocellular carcinoma: part II. Extracellular agents, hepatobiliary agents, and ancillary imaging features. Radiology 273:30-50. https://doi.org/10.1148/radiol.14132362
11. Vogl TJ, Kummel S, Hammerstingl R, Schellenbeck M, Schumacher G, Balzer T, Schwarz W, Muller PK, Bechstein WO, Mack MG, Sollner O, Felix R (1996) Liver tumors: comparison of MR imaging with Gd-EOB-DTPA and Gd-DTPA. Radiology 200:59-67. https://doi.org/10.1148/radiology.200.1.8657946
12. Ahn SS, Kim MJ, Lim JS, Hong HS, Chung YE, Choi JY (2010) Added value of gadoxetic acid-enhanced hepatobiliary phase MR imaging in the diagnosis of hepatocellular carcinoma. Radiology 255:459-466. https://doi.org/10.1148/radiol.10091388
13. Motosugi U, Ichikawa T, Sou H, Sano K, Tominaga L, Muhi A, Araki T (2010) Distinguishing hypervascular pseudolesions of the liver from hypervascular hepatocellular carcinomas with gadoxetic acid-enhanced MR imaging. Radiology 256:151-158. https://doi.org/10.1148/radiol.10091885
14. Park HJ, Kim YK, Park MJ, Lee WJ (2013) Small intrahepatic mass-forming cholangiocarcinoma: target sign on diffusion-weighted imaging for differentiation from hepatocellular carcinoma. Abdom Imaging 38:793-801. https://doi.org/10.1007/s00261-012-9943-x
15. Yang K, Cheng YS, Yang JJ, Jiang X, Guo JX (2017) Primary hepatic neuroendocrine tumors: multi-modal imaging features with pathological correlations. Cancer Imaging 17:20. https://doi.org/10.1186/s40644-017-0120-x
16. Yu JI, Kim JS, Park HC, Lim DH, Han YY, Lim HC, Paik SW (2013) Evaluation of anatomical landmark position differences between respiration-gated MRI and four-dimensional CT for radiation therapy in patients with hepatocellular carcinoma. Br J Radiol 86:20120221. https://doi.org/10.1259/bjr.20120221
17. Serste T, Barrau V, Ozenne V, Vullierme MP, Bedossa P, Farges O, Valla DC, Vilgrain V, Paradis V, Degos F (2012) Accuracy and disagreement of computed tomography and magnetic resonance imaging for the diagnosis of small hepatocellular carcinoma and dysplastic nodules: role of biopsy. Hepatology 55:800-806. https://doi.org/10.1002/hep.24746
18. Ronot M, Fouque O, Esvan M, Lebigot J, Aube C, Vilgrain V (2018) Comparison of the accuracy of AASLD and LI-RADS criteria for the non-invasive diagnosis of HCC smaller than 3cm. J Hepatol 68:715-723. https://doi.org/10.1016/j.jhep.2017.12.014
19. Bennett BM (1972) On comparisons of sensitivity, specificity and predictive value of a number of diagnostic procedures. Biometrics 28:793-800
20. Landis JR, Koch GG (1977) The measurement of observer agreement for categorical data. Biometrics 33:159-174
21. Lee YJ, Lee JM, Lee JS, Lee HY, Park BH, Kim YH, Han JK, Choi BI (2015) Hepatocellular carcinoma: diagnostic performance of multidetector CT and MR imaging-a systematic review and meta-analysis. Radiology 275:97-109. https://doi.org/10.1148/radiol.14140690
22. Obuchowski NA, McClish DK (1997) Sample size determination for diagnostic accuracy studies involving binormal ROC curve indices. Stat Med 16:1529-1542
23. Lee S, Kim KM, Lee SJ, Lee KH, Lee DY, Kim MD, Kim DY, Kim SU, Won JY (2017) Hepatic arterial damage after transarterial chemoembolization for the treatment of hepatocellular carcinoma: comparison of drug-eluting bead and conventional chemoembolization in a retrospective controlled study. Acta Radiol 58:131-139. https://doi.org/10.1177/0284185116648501
24. Suh CH, Shin JH, Yoon HM, Yoon HK, Ko GY, Gwon DI, Kim JH, Sung KB (2014) Angiographic evaluation of hepatic arterial injury after cisplatin and Gelfoam-based transcatheter arterial chemoembolization for hepatocellular carcinoma in a 205 patient

cohort during a 6-year follow-up. Br J Radiol 87:20140054. https://doi.org/10.1259/bjr.20140054
25. Kudo M (2009) Multistep human hepatocarcinogenesis: correlation of imaging with pathology. J Gastroenterol 44 Suppl 19:112-118. https://doi.org/10.1007/s00535-008-2274-6
26. Yu MH, Kim JH, Yoon JH, Kim HC, Chung JW, Han JK, Choi BI (2014) Small (</=1-cm) hepatocellular carcinoma: diagnostic performance and imaging features at gadoxetic acid-enhanced MR imaging. Radiology 271:748-760. https://doi.org/10.1148/radiol.14131996
27. Tamada T, Ito K, Sone T, Yamamoto A, Yoshida K, Kakuba K, Tanimoto D, Higashi H, Yamashita T (2009) Dynamic contrast-enhanced magnetic resonance imaging of abdominal solid organ and major vessel: comparison of enhancement effect between Gd-EOB-DTPA and Gd-DTPA. J Magn Reson Imaging 29:636-640. https://doi.org/10.1002/jmri.21689
28. Kim HS, Kim M-J, Chung J-J, Lim JS, Chung YE, Park M-S, Kim KW (2011) Focal Liver Lesion Detection in Gadoxetic Acid-enhanced Liver MRI: Effects of Scan Delay, Hepatic Function, and Magnetic Field Strength. J Korean Soc Magn Reson Med 15:226-233
29. Khan AS, Hussain HK, Johnson TD, Weadock WJ, Pelletier SJ, Marrero JA (2010) Value of delayed hypointensity and delayed enhancing rim in magnetic resonance imaging diagnosis of small hepatocellular carcinoma in the cirrhotic liver. J Magn Reson Imaging 32:360-366. https://doi.org/10.1002/jmri.22271